Electronic Supplementary Material (ESI) for Physical Chemistry Chemical Physics.

Supporting Information

Adsorption and Oxidation of Propane and Cyclopropane on $IrO_2(110)$

Rachel Martin,[1,†] Minkyu Kim,[2,†] Austin Franklin,[1] Yingxue Bian,[1] Aravind Asthagiri[2]

and Jason F. Weaver[1]

[1]Department of Chemical Engineering, University of Florida, Gainesville, FL 32611, USA

[2]William G. Lowrie Chemical & Biomolecular Engineering, The Ohio State University, Columbus, OH 43210, USA

[†] Rachel Martin and Minkyu Kim contributed equally to this work.

*To whom correspondence should be addressed, weaver@che.ufl.edu

Tel. 352-392-0869, Fax. 352-392-9513

Structure of the s-IrO_2(110) layer on Ir(100)

Bulk crystalline IrO_2 has a tetragonal unit cell with Ir atoms surrounded by an octahedral arrangement of six oxygen atoms and each oxygen atom is coordinated with three Ir atoms resulting in a trigonal plane. Figure S1 shows a top and side view of the stoichiometrically-terminated IrO_2(110) surface. The IrO_2(110) surface unit cell is rectangular with dimensions of $a = 3.16$ Å and $b = 6.36$ Å, where a and b are parallel to the [001] and $[\bar{1}10]$ directions of the IrO_2 crystal, respectively. The unit cell dimensions may also be expressed as a $a = 1.16x$ and $b = 2.34x$, where $x = 2.72$ Å is the lattice constant of Ir(100). The IrO_2(110) surface consists of alternating rows of O_{br} and Ir_{cus} that align along the [001] direction. Each of these surface species has one dangling bond due to a decrease in coordination in comparison to bulk IrO_2. H and O atoms adsorbed on top of the Ir_{cus} row are referred to as H_{ot} or O_{ot}, respectively.

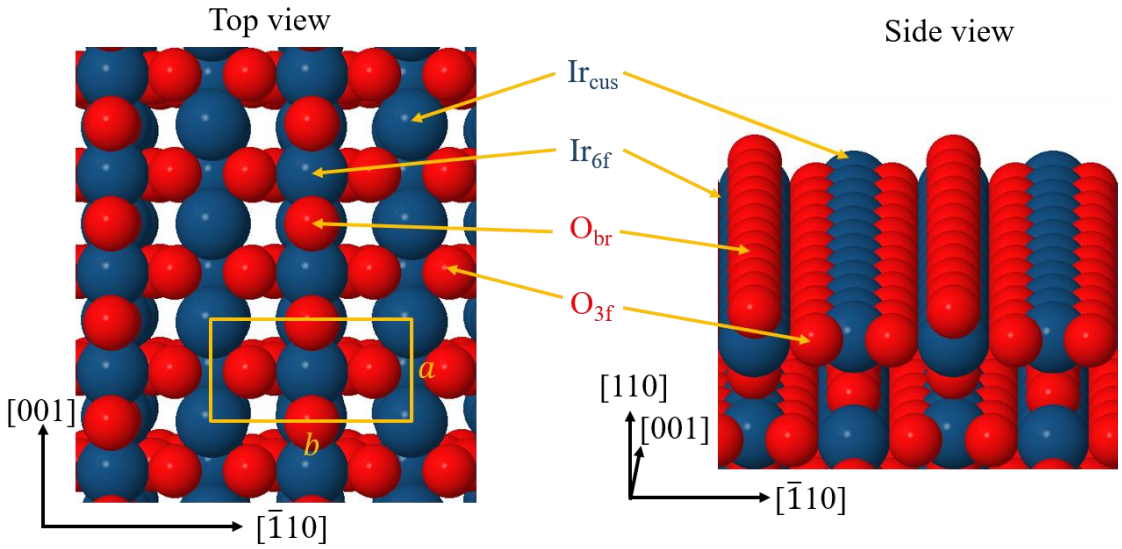

Figure S1. Model representation of top and side view of stoichiometric IrO_2(110) structure. The red and blue atoms represent O and Ir atoms, respectively. Rows of Ir_{cus}, Ir_{6f}, O_{br}, O_{3f} along the [001] crystallographic direction are indicated. The unit cell dimensions *a* and *b* are parallel to the [001] and $[1\bar{1}0]$ directions of the IrO_2 crystal.

Measurement of product yields

We estimate atomic oxygen coverages by scaling integrated O_2 TPD spectra with those obtained from a saturated (2×1)-O layer containing 0.50 ML of O-atoms and prepared by exposing the Ir(100)-(5×1) surface to O_2 in UHV.[1] To estimate hydrogen coverages, we scaled integrated hydrogen desorption spectra by an integrated TPD spectrum collected from a saturated Ir(100)-(5×1)-H layer containing 0.80 ML of atomic hydrogen that we prepared by adsorbing hydrogen to saturation on the Ir(100)-(5×1) surface at 300 K.[2] We performed TPRS experiments of CO oxidation on saturated O-covered Ir(100) to estimate the CO_2 desorption yields. Specifically, we collected O_2 and CO_2 TPRS spectra after exposing a (2×1)-O layer to a sub-saturation dose of CO and assuming that the CO_2 yield is equal to the difference between the initial (0.50 ML) and final coverages of oxygen as determined from the O_2 TPRS yield. To estimate CO desorption yields, we scaled integrated CO desorption spectra by an integrated TPD spectrum collected from a saturated c(2×2) layer containing 0.50 ML of CO that we prepare by adsorbing CO to saturation on Ir(100)-(1×1) at 300 K.[1, 3-4]

We performed TPRS experiments of hydrogen oxidation on partially O-covered Ir(100) to estimate the water desorption yields. In these experiments, we first collected O_2 and CO_2 TPRS spectra after exposing a (2×1)-O layer to a sub-saturation dose of CO and assuming that the oxygen remaining on Ir(100) is equal to the difference between the initial oxygen coverage in the (2×1)-O layer (0.50 ML) and the CO_2 yield determined from the CO_2 TPRS spectrum. We then collected O_2 and H_2O TPRS spectra after exposing the partially O-covered Ir(100) surface generated from the first step to a saturation dose of hydrogen and assuming that the water yield is equal to the difference between the initial and finial coverage of oxygen determined from the O_2 TPRS yield. We repeat these calibration TPRS experiments to ensure accuracy in our estimates of

desorption yields. We estimated C_3H_8 and c-C_3H_6 coverages by scaling the intensity-to-yield conversion factors determined for O_2 with relative sensitivity factors (RSF) estimated for the mass spectrometric detection of these gases. We used a reported RSF value to compute the C_3H_8 desorption yield,[5] and estimated the RSF for c-C_3H_6 by scaling the C_3H_8 RSF with the ratio of electron-impact ionization cross sections for c-C_3H_6 and C_3H_8 (~0.81) reported in the literature.[6]

TPRS spectra as a function of the C_3H_8 coverage on IrO_2(110)

Figure S2 shows H_2O, CO, C_3H_8 and CO_2 TPRS spectra obtained as a function of the initial C_3H_8 coverage generated on IrO_2(110)/Ir(100) at 90 K. We represent the H2O and C3H8 TPRS spectra using the measured intensities of the *m/z* = 18 and 29 fragments, respectively, and represent the CO and CO_2 TPRS spectra with the measured intensities of the *m/z* = 28 and 44 fragments after removing the low-temperature features generated by C_3H_8 fragmentation in the ionizer. We discontinued each TPRS experiment at 650 K before the H_2O TPRS feature returned to the baseline. As described in the main manuscript, limiting the final temperature to 650 K allows us to subsequently regenerate the IrO_2(110) surface by O_2 treatment in UHV and thus collect TPRS data efficiently using the same oxide film. The data shows that a C_3H_8 TPD peak at ~205 K, attributed to desorption of an adsorbed C_3H_8 σ-complex, first appears after adsorbing just over 0.20 ML of propane, and the CO_x products yields begin to plateau. At a total C_3H_8 coverage of 0.31 ML, the propane TPD spectra exhibit a saturated peak at 205 K and a new peak at ~150 K that we attribute to C_3H_8 associated with O_{br} atoms of the surface. This latter peak appears to downshift to ~140 K and intensify significantly at higher propane coverage, while the peak at 205 K remains saturated.

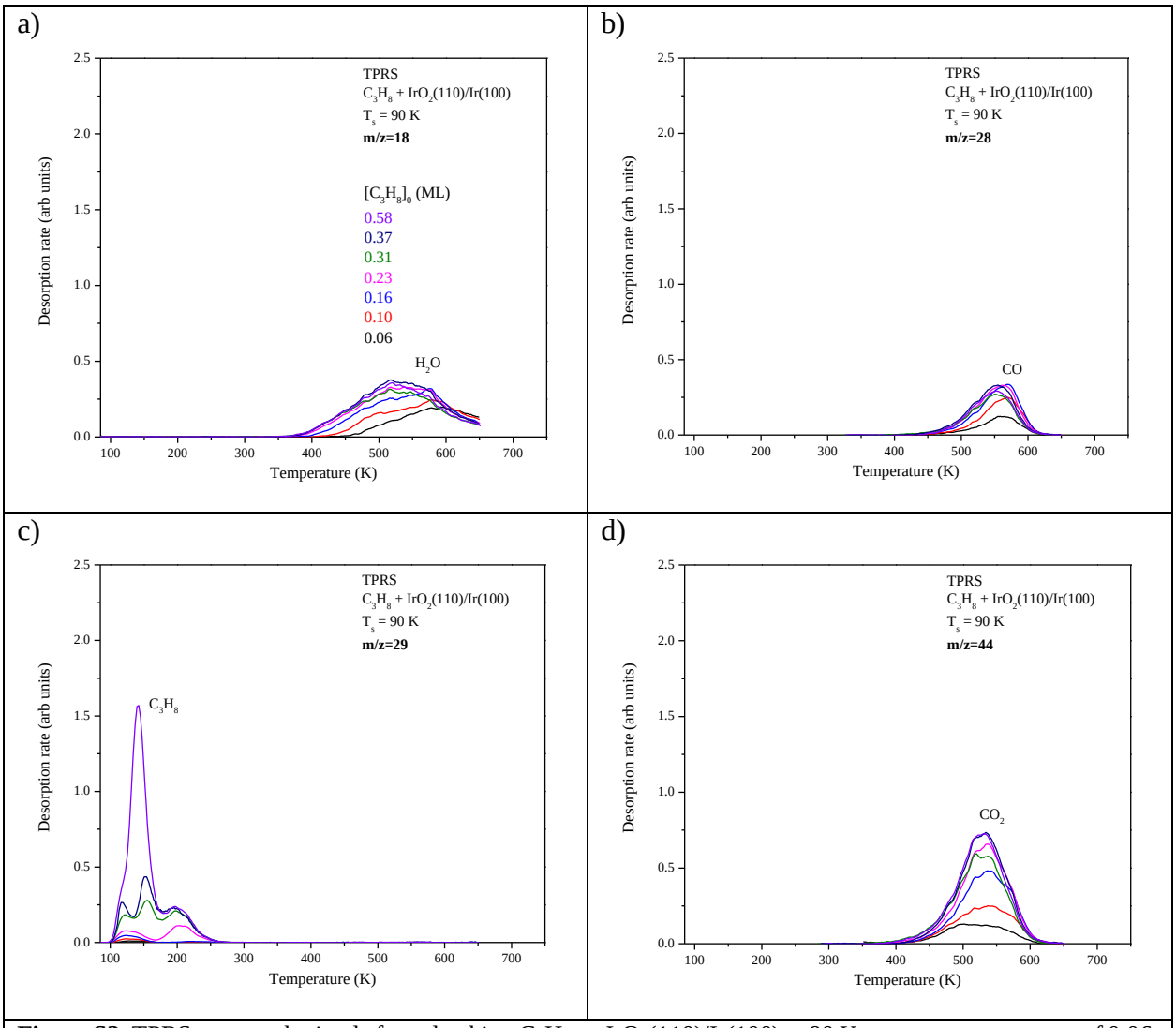

Figure S2. TPRS spectra obtained after adsorbing C_3H_8 on IrO_2(110)/Ir(100) at 90 K to generate coverages of 0.06, 0.10, 0.16, 0.23, 0.31, 0.37 and 0.58 ML. TPRS traces are shown for a) H_2O, b) CO, c) C_3H_8 and d) CO_2.

TPRS spectra as a function of the c-C_3H_6 coverage on IrO_2(110)

Figure S3 shows H_2O, CO, c-C_3H_6 and CO_2 TPRS spectra obtained as a function of the initial C_3H_8 coverage generated on IrO_2(110)/Ir(100) at 90 K. We represent the H_2O and c-C_3H_6 TPRS spectra using the measured intensities of the *m/z* = 18 and 42 fragments, respectively, and represent the CO and CO_2 TPRS spectra with the measured intensities of the *m/z* = 28 and 44 fragments after removing the low-temperature features generated by c-C_3H_6 fragmentation in the ionizer. We discontinued each TPRS experiment at 650 K before the H_2O TPRS feature returned to the baseline. The c-C_3H_6 TPD spectra first exhibit a peak near 145 K at a total c-C_3H_6 coverage of 0.44 ML, with this peak intensifying and slightly downshifting with increasing c-C_3H_6 coverage. As discussed in the main manuscript, we attribute the peak near 145 K to c-C_3H_6 that is associated with O_{br} atoms, and conclude that c-C_3H_6 σ-complexes form in high coverages on IrO_2(110) but that they all the complexes oxidize and thus do not generate a distinct c-C_3H_6 TPD peak.

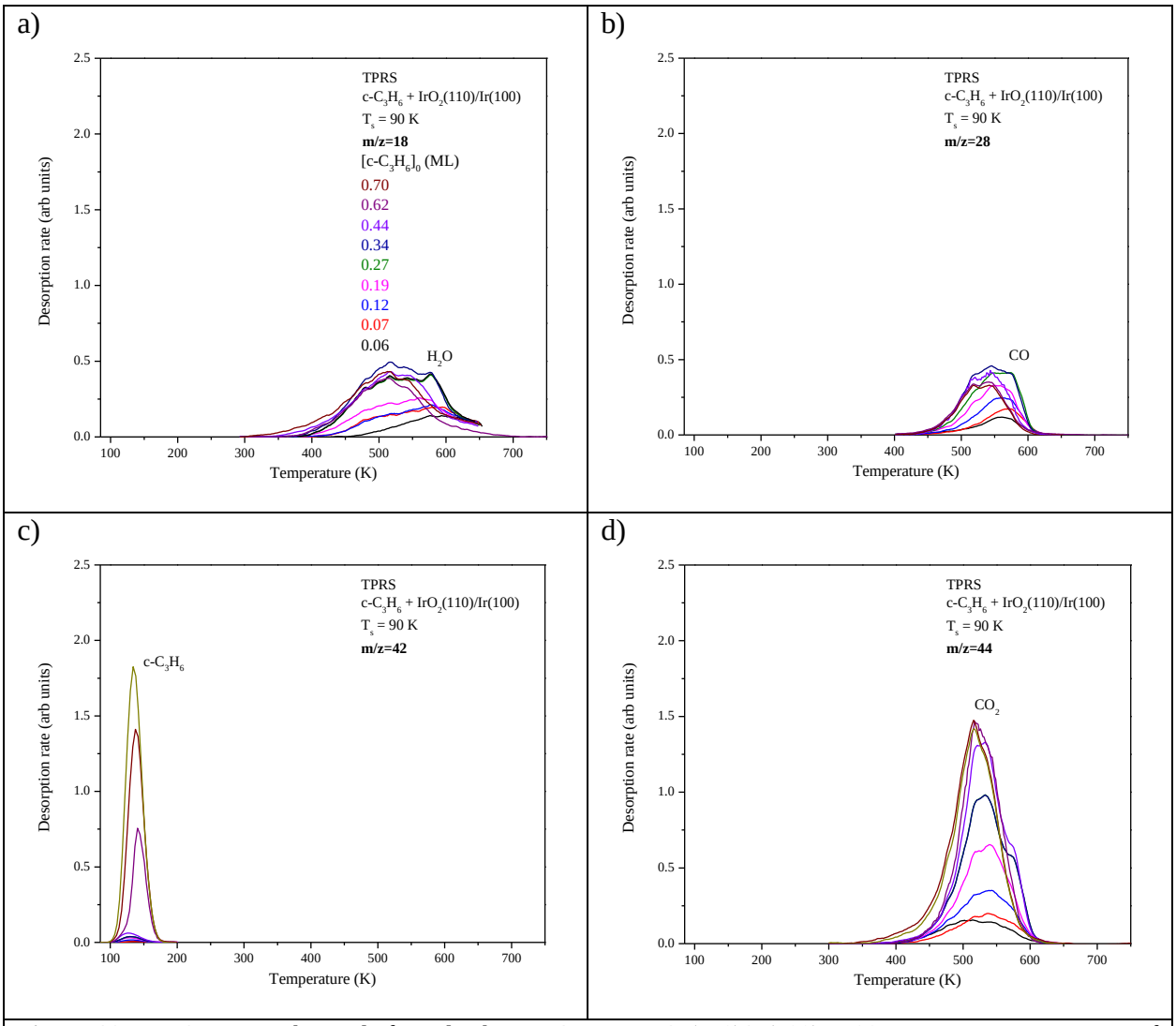

Figure S3. TPRS spectra obtained after adsorbing c-C_3H_6 on IrO_2(110)/Ir(100) at 90 K to generate coverages of 0.06, 0.07, 0.12, 0.19, 0.27, 0.34, 0.44, 0.62 and 0.70 ML. TPRS traces are shown for a) H_2O, b) CO, c) c-C_3H_6 and d) CO_2.

Configurations of C_3H_8 σ-complexes on IrO_2(110) predicted by DFT-D3

Figure S4 shows the four configurations of C_3H_8 σ-complexes on IrO_2(110) identified with DFT-D3. DFT-D3 predicts that the p-2η^1 complex is the favored adsorbed configuration of C_3H_8 on IrO_2(110) surface.

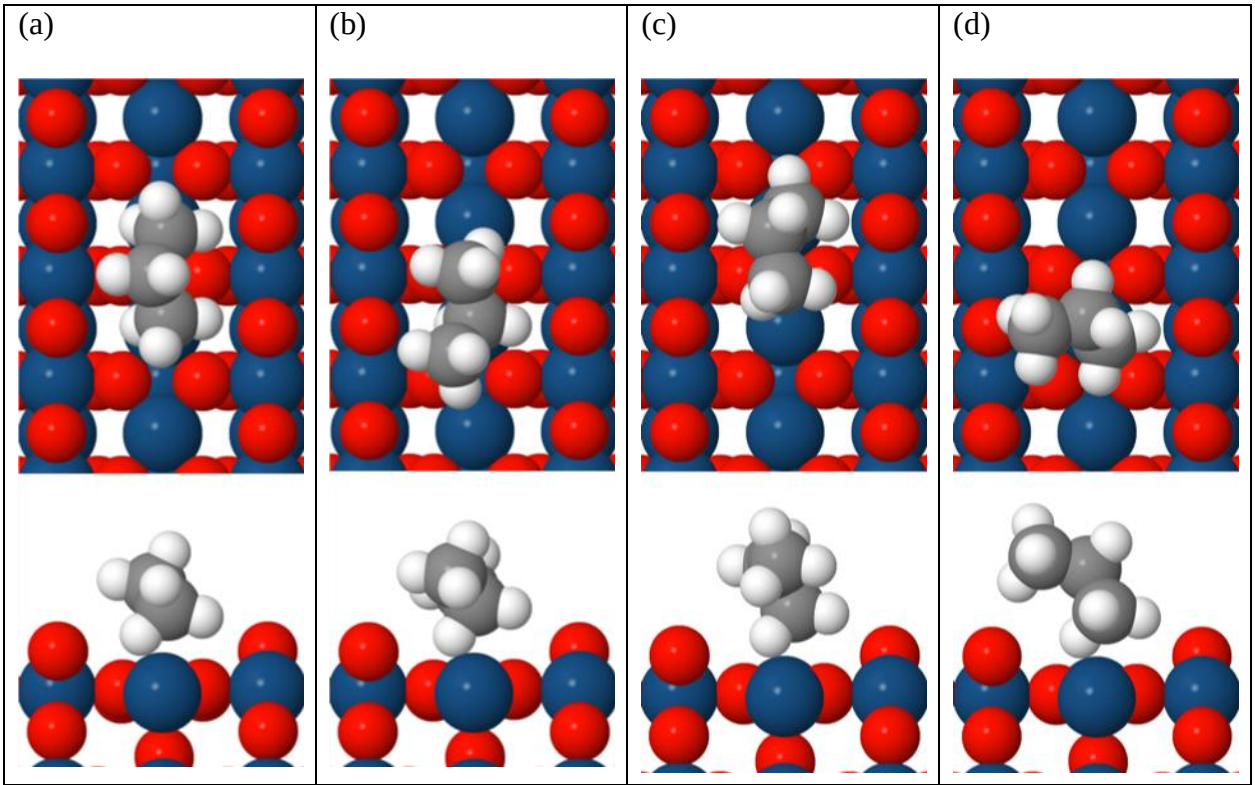

p-2η^1 E_b = 145 kJ/mol	s-η^1 E_b = 111 kJ/mol	p-η^1-|| E_b = 96 kJ/mol	p-η^1-⊥ E_b = 91 kJ/mol

Figure S4. Molecular configurations of the stable C_3H_8 (a) p-2η^1, (b) s-η^1, (c) p-η^1-|| and (d) p-η^1-⊥ complexes on IrO_2(110) as determined using DFT-D3.

Configurations of c-C_3H_6 σ-complexes on IrO_2(110) predicted by DFT-D3

Figure S5 shows the four configurations of c-C_3H_6 σ-complexes on IrO_2(110) identified with DFT-D3. DFT-D3 predicts that the $2\eta^1$ complex is the favored adsorbed configuration of c-C_3H_6 on IrO_2(110) surface.

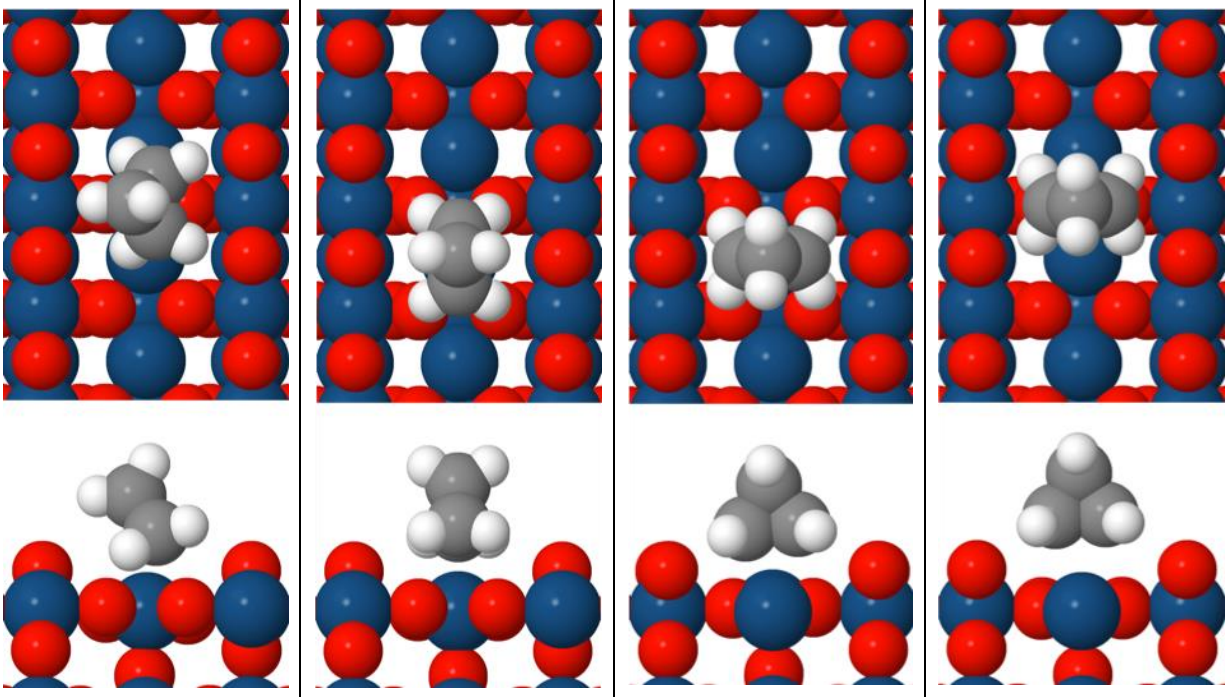

$2\eta^1$	η^2(C,C)-‖	η^2(C,C)-⊥	η^2(C,C)-⊥ (bridge)
E_b = 126 kJ/mol	E_b = 97 kJ/mol	E_b = 82 kJ/mol	E_b = 46 kJ/mol

Figure S5. Molecular configurations of c-C_3H_6 complexes on IrO_2(110) as determined using DFT-D3. The $2\eta^1$ configuration shown in (a) has no imaginary frequencies and thus corresponds to a minimum in the potential energy surface, whereas the configurations shown in (b), (c) and (d) each have one or two imaginary frequencies, indicating that these structures occur at saddle points on the potential energy surface.

Pathways for dehydrogenation of the bidentate C_3H_6 intermediate on IrO_2(110)

Figure S6 compares pathways computed for cleavage of a C-H bond from the different CH_x groups of the C_3H_7(ad) species, and also lists the thermochemical barriers for subsequent C_3H_6(g) generation. Our calculations predict that C-H bond cleavage of the CH_3 group of C_3H_7(ad), affording the $CH_2CH_2CH_2$(ad) species, is kinetically and thermodynamically preferred over C-H bond cleavage of the CH_2 groups. Cleavage of a C-H bond of the interior CH_2 group to generate an adsorbed propylene species (CH_3CHCH_2) is kinetically and thermodynamically disfavored relative to the other C_3H_7(ad) dehydrogenation reactions (Figure 8b, blue). Cleavage of a C-H bond of the terminal CH_2 group to produce adsorbed CH_3CH_2CH(ad) has a barrier of only 48 kJ/mol (Figure 8b, black), and could be kinetically competitive with C_3H_7(ad) dehydrogenation to $CH_2CH_2CH_2$(ad) for which the barrier is 41 kJ/mol. The resulting CH_3CH_2CH(ad) species would preferentially dehydrogenate if O_{br} atoms are available. Interestingly, conversion of the CH_3CH_2CH(ad) species to gaseous propylene has a minimum barrier that is lower than the barriers for O_{br} regeneration (160 vs. 220-260 kJ/mol), suggesting the possibility of propylene formation at high HO_{br} coverages. However, C_3H_7(ad) dehydrogenation to CH_3CH_2CH(ad) has a small exothermicity of 22 kJ/mol, and thus a barrier of only 70 kJ/mol is required for H-transfer to CH_3CH_2CH(ad) to regenerate C_3H_7(ad) (Figure 8b, black). In contrast, a much larger barrier (127 kJ/mol) must be overcome for the $CH_2CH_2CH_2$(ad) species to be hydrogenated to C_3H_7(ad). The net effect is that the $CH_2CH_2CH_2$(ad) species will be the dominant product of C_3H_7(ad) dehydrogenation on IrO_2(110), and its formation ultimately results in extensive oxidation to CO_x as O_{br} atoms are regenerated.

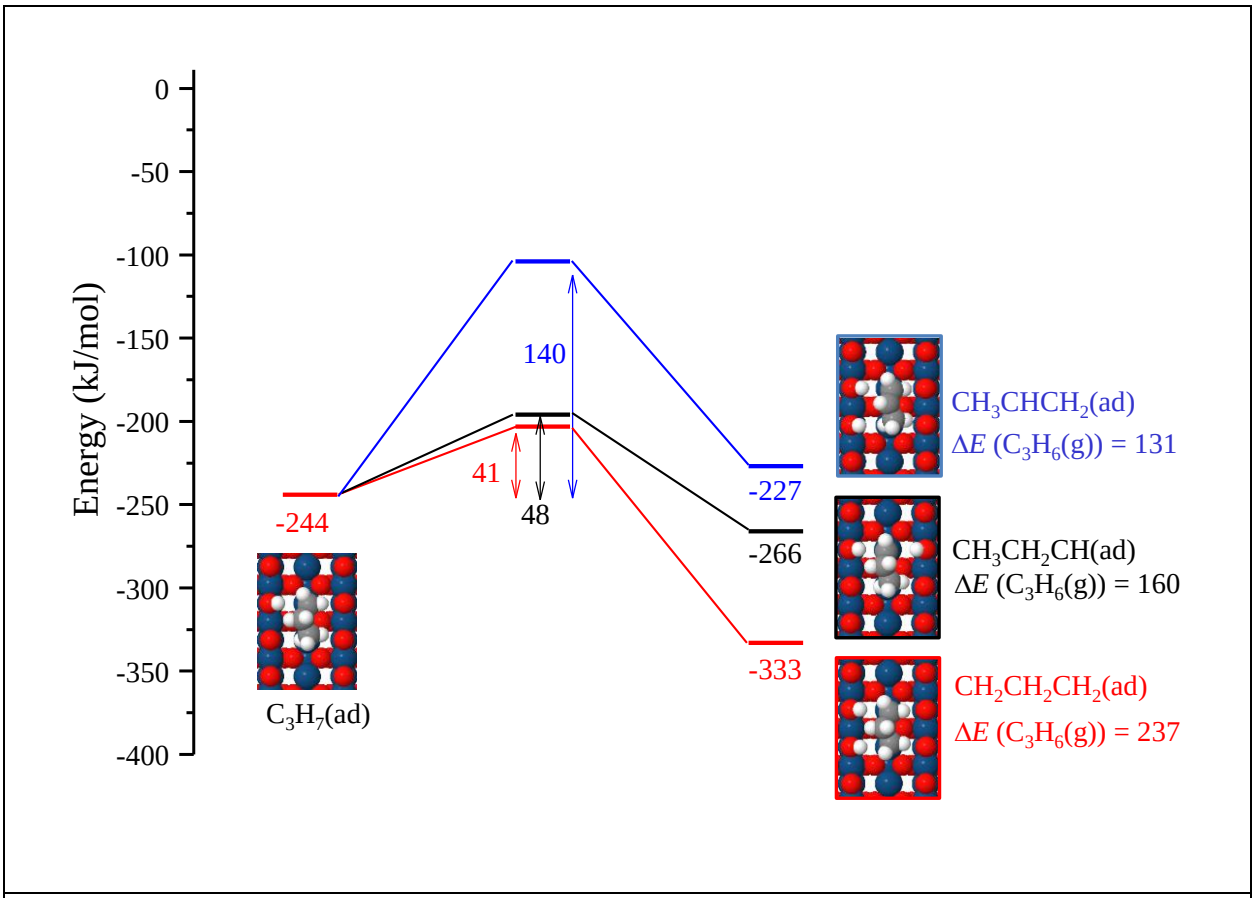

Figure S6: Comparison of computed pathways for cleavage of a C-H bond from each CH_x group of the C_3H_7(ad) species on IrO_2(110), including the terminal (black) and interior (blue) CH_2 groups and the CH_3 group (red).

1. Anic, K.; Bulchtiyarov, A. V.; Li, H.; Rameshan, C.; Rupprechter, G., "CO Adsorption on Reconstructed Ir(100) Surfaces from UHV to mbar Pressure: A LEED, TPD, and PM-IRAS Study". *J. Phys. Chem. C* **2016**, *120*, 10838-10848.
2. Arman, M. A.; Klein, A.; Ferstl, P.; Valookaran, A.; Gustafson, J.; Schulte, K.; Lundgren, E.; Heinz, K.; Schneider, A.; Mittendorfer, F.; Hanuner, L.; Knudsen, J., "Adsorption of hydrogen on stable and metastable Ir(100) surfaces". *Surf. Sci.* **2017**, *656*, 66-76.
3. Kisters, G.; Chen, J. G.; Lehwald, S.; Ibach, H., "Adsorption of Co on the Unreconstructed and Reconstructed Ir(100) Surface". *Surf. Sci.* **1991**, *245*, 65-71.
4. Lerotholi, T. J.; Held, G.; King, D. A., "Phase mixing and phase separation accompanying the catalytic oxidation of CO on Ir{100}". *Surf. Sci.* **2007**, *601*, 1285-1295.
5. Relative Sensitivity: RS measurements of gases *Application Note 282*, https://www.hiden.de/wp-content/uploads/pdf/RS_Measurement_of_Gases_-_Hiden_Analytical_App_Note_282.pdf.
6. Nishimura, H.; Tawara, H., "Total Electron-Impact Ionization Cross-Sections for Simple Hydrocarbon Molecules". *Journal of Physics B-Atomic Molecular and Optical Physics* **1994**, *27*, 2063-2074.